

Ahmad K. Ahmad ¹
 Firas A. Abdulrahman ²
 Roaa Ayad Aldoori ³

¹ College of Engineering,
 Al-Nahrain University,
 Baghdad, IRAQ

² Mobile communication and
 computing engineering
 department,
 College of Engineering,
 University of Information and
 Communication Technology,
 Baghdad, IRAQ

³ College of Engineering,
 Al-Iraqia University,
 Baghdad, IRAQ



Design of Einzel Electrostatic Lenses Using Inverse Schiske's Model

This paper examines the computational design of an electrostatic Einzel lens utilizing the inverse Schiske's model with certain magnification conditions. The electrostatic lens potential distribution has been characterized by an analytical function referred to as the inverse Schiske model. By solving the paraxial ray equation with the Runge-Kutta technique of fourth order, the charged particle beam trajectory and its derivatives via the lens have been determined. One can determine the proposed electrostatic lens optical properties, for instance, magnification, focal properties, and aberrations (spherical and chromatic), from knowing the axial potential distributions of the Einzel lens' and its first and second derivatives, as well as the beam trajectory and its derivatives. Based on our findings, we can infer that the constant k substantially affects the aberration values, with the best results happening at $k = 0.1$ for constants ($V_0 = 1V$ and $a = 0.025$) with a 10mm lens length. Also, the form of the suggested lens' electrodes is calculated.

Keywords: Electrostatic lens; Spherical aberration; Paraxial ray equation

Received: 25 February 2024; **Revised:** 24 March 2024; **Accepted:** 31 March 2024

1. Introduction

Einzel lenses are distinguished by having constant potential $U_1=U_3$ on both the object and image sides, whereas the center electrode has a separate potential U_2 . Consequently, they are utilized when simply focusing is necessary. Nevertheless, the energy of the beam needs to be conserved. Einzel lenses are symmetrical cylinder electrodes, where the lens's center for both foci. Consequently, they are commonly known as symmetrical round lenses [1]. Due to their adaptability and the fast development of contemporary instrumentation, Einzel lenses are finding growing usage in various scientific and technological fields [2-7].

The current work aims to discover a more straightforward expression to represent the potential axial distribution of the Einzel lens with bearable aberrations. The inverse Schiske's recommended model [8] has been used to illustrate the Einzel lens's potential field distribution as follows:

$$U(z) = \frac{1}{V_0(1 - \frac{k^2}{1 + (\frac{z}{a})^2})} \quad (1)$$

Equation (1) may reflect the accelerator mode potential distribution along an Einzel lens' optical axis, where z is the lens optical axis, and (a , k , and V_0) are parameters by which the shape and symmetry of the lens and the value of the voltage inside the lens can be controlled. A non-relativistic electron beam traveling close to the axis in a symmetrical cylindrical electrostatic field of a lens system can be controlled by the equations of motion called the paraxial ray equation [1,9].

$$r'' + r' \frac{U'}{2U} + r \frac{U''}{4U} = 0 \quad (2)$$

where U' and U'' are the axial potential's first and second derivatives, respectively. The primes signify a derivative for z , and r denotes beam radial displacement from the optical axis z .

Equation (2) is a linear and homogeneous second-order differential equation. Knowing the potential distribution along the z -axis $U(z)$, you also know the factors in front of r'' , r' , and r [10]. To calculate the aberration coefficients, spherical and chromatic, the following equations are used [11,12].

The electrode shapes are found by using a synthesis approach where the profiles of the electrodes correspond to the axial field distribution found with the aid of the following equation [12,13]:

$$R = 2 \left(U(z) - \frac{U(r,z)}{U''(z)} \right)^{0.5} \quad (5)$$

The Wolfram Mathematica program is used in the design of the electrostatic einzel lens which is described in previous research [14].

2. Results and Discussion

An Einzel lens with a center electrode at a higher voltage than the two outer electrodes is seen in Fig. (1a) called the axial potential distribution. Away from the lens terminals, there is a field-free region, i.e. there is no force acting on the trajectory of the charged particle beam, that is, a straight line. This indicates that there is no electric field outside the lens because the potential distribution $U(z)$ is constant at the boundaries, and therefore its first derivative $U'(z)$

is zero. The lens contains three electrodes since the potential second derivative $U''(z)$ has two inflection points [12]. The axial potential distribution $U(z)$ for the inverse Schiske's electrostatic einzel lens is shown in Fig. (2a) for different values of V_0 at constant ($a=0.025$, $k=0.7$), (2b) different values of a , at constant ($V_0=1$, $k=0.3$), and (2c) different values of k at constant ($V_0=1$, $a=0.025$).

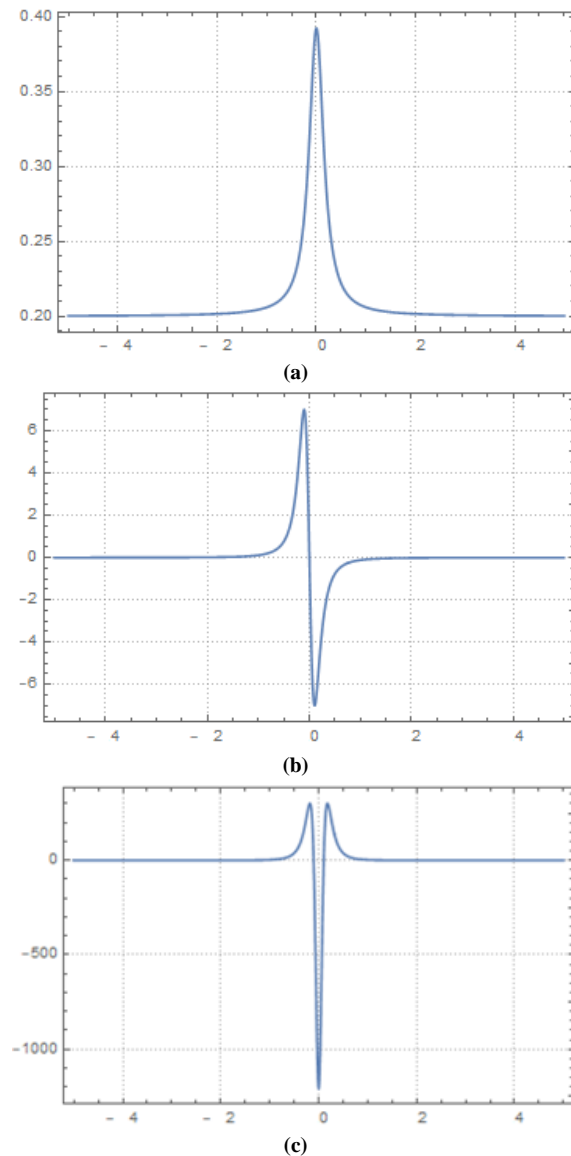


Fig. (1) (a) $U(z)$, (b) $U'(z)$, (c) $U''(z)$. The axial potential distribution and its first and second derivatives respectively, for inverse Schiske's model electrostatic Einzel lens for ($V_0=5V$, $a=0.025$, $k=0.7$ and $L=10mm$)

From Fig. (2), one can notice that the values of the maximum potential decrease as V_0 increases when a and k are constant as shown in Fig. (2a). When changing values of a when keeping V_0 and k are constants, we notice that the full-width at half maximum (FWHM) increases with increasing values of a as shown in Fig. (2b). Also, when increasing values of k , with constants a and V_0 , the values of the maximum potential decrease as shown in Fig. (2c).

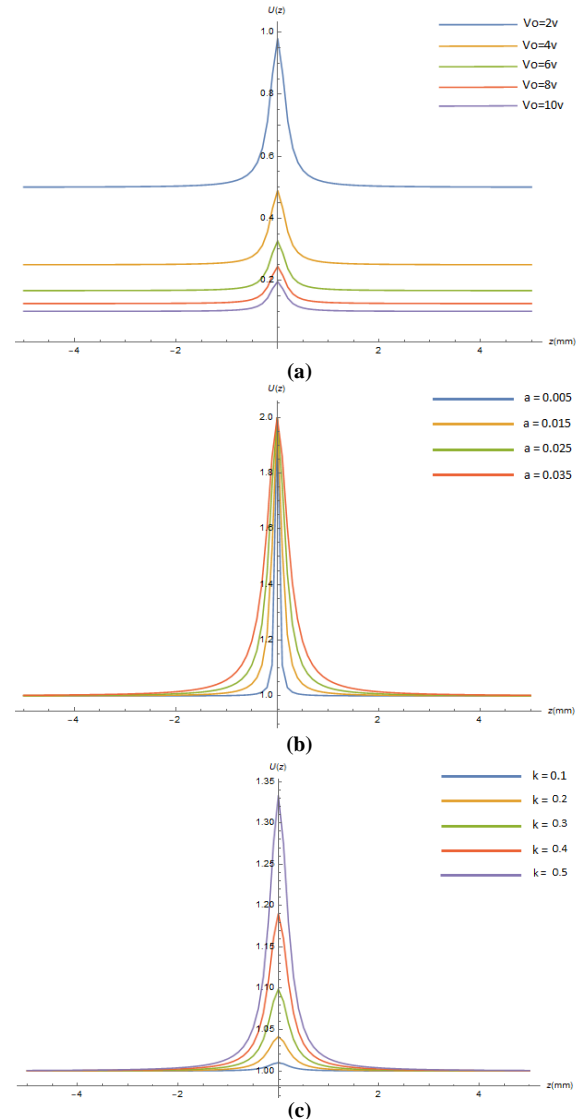


Fig. (2) The potential field $U(z)$ axial distribution for inverse Schiske's electrostatic Einzel lens for (a) different value of V_0 at constant ($a=0.025$, $k=0.7$) (b) different values of a , at constant ($V_0=1$, $k=0.3$) and (c) different values of k , at constant ($V_0=1$, $a=0.025$)

Figures (3a) and (4a) show the electron beam's course in the electrostatic einzel lens field at zero and infinite magnification, respectively, at various values of V_0 . Considering that (a and k) are constants. The trajectory of the electron beams gradient increases as V_0 value increases. At $a=0.025$ and $k=0.2$, whereas the other electron beam paths (various values of V_0) shifted downward, the electron beams intersect the lens optical axis.

Figures (3b) and (4b) show the electron beam trajectory for various values of a ; it is seen that the trajectory beam tends to be straight with the increasing value of a . As increasing of the constant a , the trajectory converges until they become constants for large values of a . Figures (3c) and (4c) show the electron beam trajectory for constant values ($V_0=1V$, $a=0.025$) and various values of k . It is observed that

with increasing the values of k , the trajectory shifted down and got closer to the optical axis z .

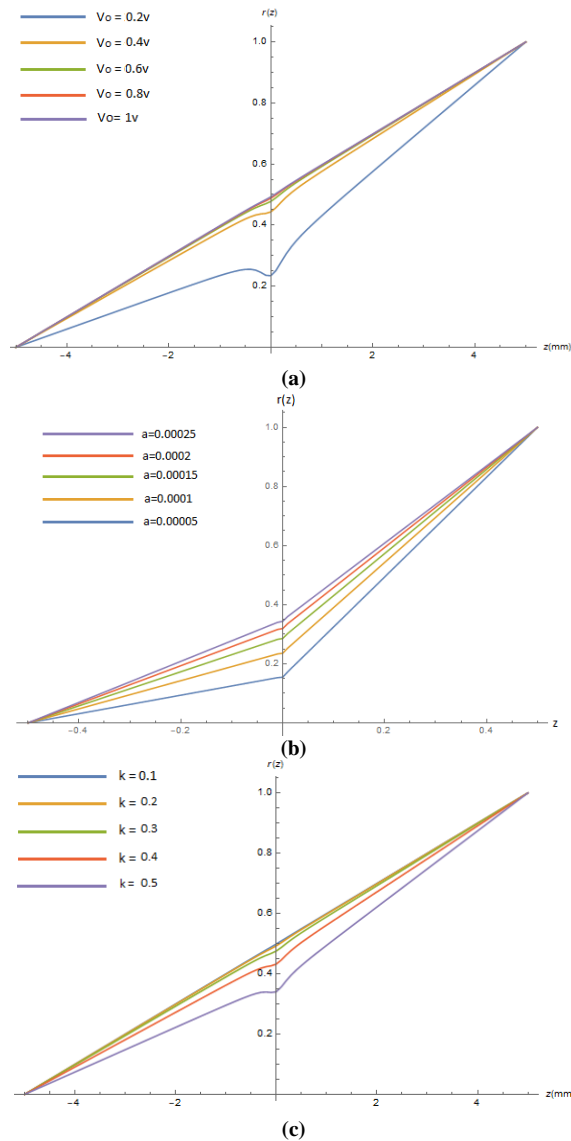


Fig. (3) The trajectories of electron beam for the einzel electrostatic lens under infinite magnification conditions at diverse values of (a) V_0 , (b) a , and (c) k

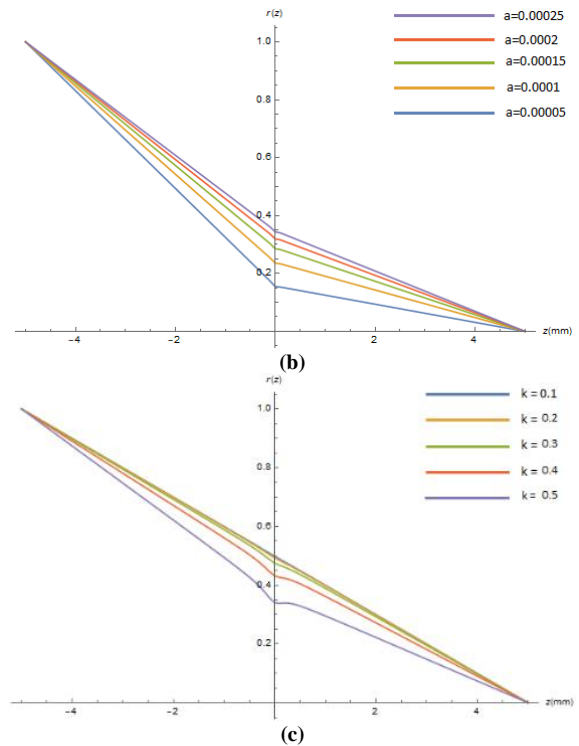
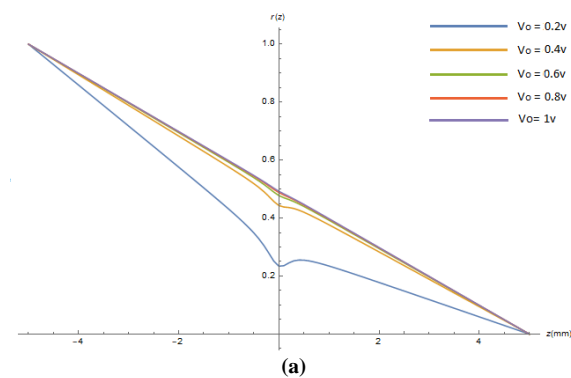


Fig. (4) The trajectories of electron beam for the einzel electrostatic lens under zero magnification conditions at diverse values of (a) V_0 , (b) a , and (c) k

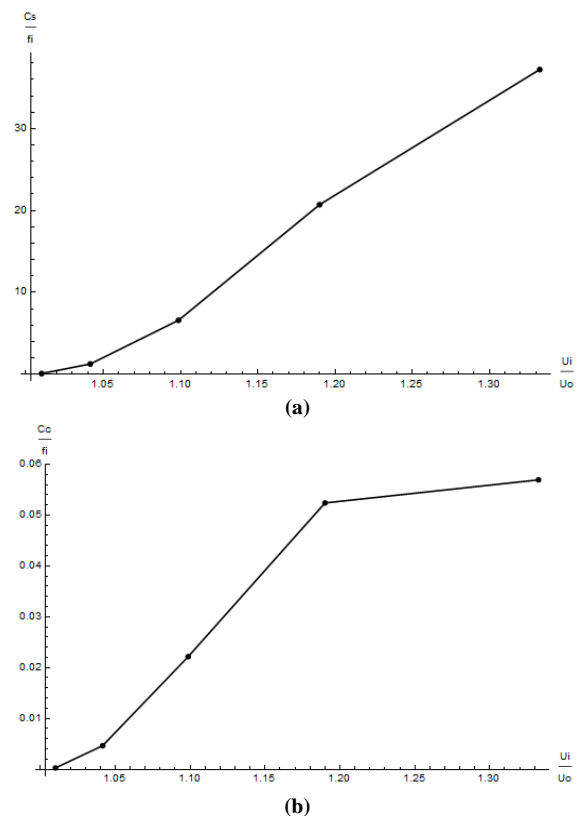


Fig. (5) (a) Spherical and (b) Chromatic relative aberrations coefficients respectively, versus U_i/U_0 for zero magnification conditions at $a=0.025$ and $V_0=1V$

Figure (5) displays the U_i/U_0 voltage ratio-dependent image-side relative spherical and chromatic aberration coefficients, C_s/f_i and C_c/f_i ,

respectively, for the electrostatic Einzel lens operating at zero magnification at various values of k (since the voltage ratio changes only with the changing the constant k). According to this figure, as k increases, or as the ratio U_i/U_0 increases, so do the relative spherical and chromatic aberration coefficients.

In Fig. (6), the object side C_s/f_o and C_o/f_o were computed for a range of the voltage ratio U_i/U_0 at various values of k . Figure (6) shows that C_s/f_o and C_o/f_o increase with increasing U_i/U_0 . From the last to figures one can conclude that low values of C_s/f_o , C_o/f_o , C_s/f_i and C_o/f_i are achieved at low values of k .

Table (1) shows the image and object side's relative chromatic and spherical aberration coefficients for different values of k at constant $a=0.025$ and $V_0=1V$, from this table, one may see that the relative chromatic and spherical aberration coefficients increase with increasing the values of k as shown in the figures (5) and (6).

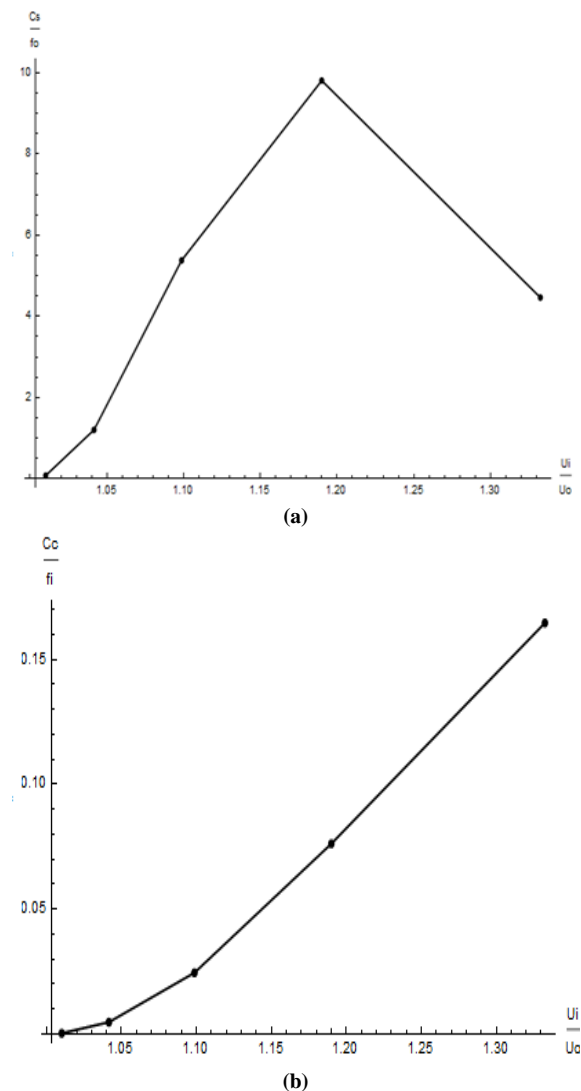


Fig. (6) The relative (a) Spherical and (b) Chromatic aberration coefficients respectively, versus U_i/U_0 at diverse values of k under infinite magnification conditions with $a=0.025$ and $V_0=1V$

Table (1) The image and object side relative chromatic and spherical aberration coefficients for diverse values of k

k	f	U_i/U_0	C_s/f_i	C_o/f_i	C_s/f_o	C_o/f_o
0.1	1.000	1.010	0.075	0.0003	0.075	0.0002
0.2	1.004	1.040	1.243	0.0046	1.200	0.0047
0.3	1.026	1.090	6.582	0.0221	5.830	0.0245
0.4	1.102	1.190	20.172	0.0524	9.812	0.0762
0.5	1.349	1.333	37.323	0.0569	4.463	0.1650

The electrode shapes are determined using the synthesis method, i.e., the shape of the electrodes corresponds to the axial potential distribution was calculated with the aid of Eq. (5). Figure (7) depicts the two-dimensional electrostatic forms that represent the einzel lens. From this figure, we can recognize the shape of the electrodes by rotating these shapes around the optical axis with the boor diameter of the central electrode equal to 2.8 mm.

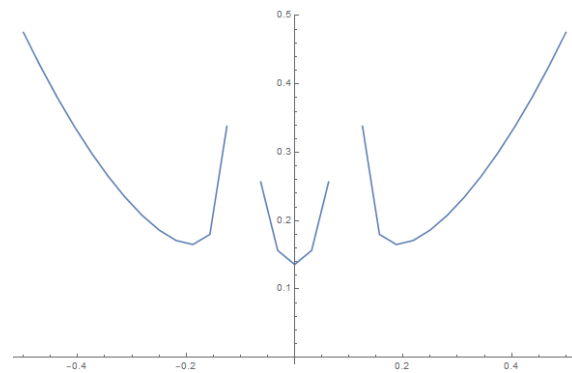


Fig. (7) The Einzel lens's three-electrodes correspond to the axial distribution of the constant ($V_0=1V$ and $a=0.025$, $k=0.3$ and $L=10mm$)

3. Conclusion

The current study demonstrates that several types of electrostatic lenses with tiny aberrations can be designed and operated at varied potential ratios. It has been discovered that utilizing the invers Schiske's model, which can be utilized to solve the paraxial ray equation of charged particles, it is possible to create an Einzel lens with low aberration and the shortest course of the electron trajectory. The results show that the aberration coefficient decreases as the constant k decreases, where the best outcome occurs at the constant k are equal to 0.1 with constants ($V_0=1V$, $a=0.025$) for lens length equal to 10mm.

References

- [1] B. Paszkowski, "Electron Optics", Itffe Book (London, 1968).
- [2] R.R.A. Syms, L. Michelutti and M.M. Ahmad, "Two-dimensional microfabricated electrostatic einzel lens", *Sens. Actuat. A*, 107(3) (2003) 285-295.
- [3] M.H. Rashid, "Simple analytical method to design electrostatic einzel lens", *Proc. DAE Symp. on Nucl. Phys.*, 56 (2011) 1132-1133.

- [4] O. Sise, M. Ulu and M. Dogan, "Multi-element cylindrical electrostatic lens systems for focusing and controlling charged particles", *Nucl. Instrum. Meth. A*, 554 (2005) 114-131.
- [5] K. Ho-Seob et al., "Arrayed microcolumn operation with a wafer-scale Einzel lens", *Microelectron. Eng.*, 7879 (2005) 55-61.
- [6] S.N. Mazhir, "Generated and shifted of Ion beams By Electrostatic Lenses (Einzel lens)", *Baghdad Sci. J.*, 12(5) (2015) 814-821.
- [7] A.K. Ahmad and B.F. Abd-Alghane, "Design and analysis of the optical properties of electrostatic unipotential lens (einzel lens)", *J. Opt.*, 52 (2023) 1704-1709.
- [8] A. Amer and A.K. Ahmad, "Differential algebraic description for aberrations analysis of typical electrostatic einzel lens", *Optik*, 168 (2018) 112-117.
- [9] Grivet, "**Electron Optics**", 2nd ed., Elsevier Ltd. (1972).
- [10] J. Szep and M. Szilagy, "A novel approach to the synthesis of electrostatic lenses with minimized aberrations", *IEEE Trans. Electron Dev.*, 35(7) (1988) 1181-1183.
- [11] M. Szilagy and J. Szepa, "Optimum design of electrostatic lenses", *J. Vac. Sci. Technol. B*, 6(1) (1988) 953-957.
- [12] A.K. Ahmad, S.M. Juma and A.A. Al-Tabbakh, "Computer aided design of an electrostatic FIB system", *Indian J. Phys.*, 76B(6) (2002) 711-714.
- [13] M. Szilagy, "Reconstruction of electrodes and pole pieces from optimized axial field distributions of electron and ion optical systems", *Appl. Phys. Lett.*, 45(5) (1984) 499-501.
- [14] A.K. Ahmad and F.A. Abdularhman, "Design of Einzel Electrostatic Lenses Using Schiske's Model", *AIP Conf. Proc.*, 2830 (2023) 040012.

$$C_{so} = \frac{U_o^{-1/2}}{16r_o'^4} \int_{zo}^{zi} \left(\frac{5}{4} \left(\frac{U''}{U} \right)^2 + \frac{5}{24} \left(\frac{U'}{U} \right)^4 + \frac{14}{3} \left(\frac{U'}{U} \right)^3 \frac{r'}{r} - \frac{3}{2} \left(\frac{U'}{U} \right)^2 \frac{r'^2}{r^2} \right) \sqrt{U} r^4 dz \quad (3)$$

$$C_{co} = \frac{\sqrt{U_o}}{r_o'^2} \int_{zo}^{zi} \left(\frac{1}{2} \left(\frac{U'}{U} \right) r' + \frac{1}{4} \left(\frac{U''}{U} \right) r \right) \frac{r}{\sqrt{U}} dz \quad (4)$$

where C_{so} and C_{co} represent the spherical and chromatic aberration, respectively.